

Biochar-Induced Priming Effects in Young and Old Poplar Plantation Soils

Weiwei Lu^{1,*}, Yirui Zhang¹, Yixian Yao¹, Yuying Wu¹, Han Y. H. Chen², Hailin Zhang³, Jia Yu⁴,
Caiqin Shen⁵, Qi Liu⁶ and Honghua Ruan^{1,*}

¹College of Biology and the Environment, Co-Innovation Center for Sustainable Forestry in Southern China, Nanjing Forestry University, Nanjing, 210037, China

²Faculty of Natural Resources Management, Lakehead University, Thunder Bay, ON, P7B 5E1, Canada

³Department of Plant and Soil Sciences, Oklahoma State University, Stillwater, OK, 74078, USA

⁴Advanced Analysis and Testing Center, Nanjing Forestry University, Nanjing, 210037, China

⁵State Owned Forest Farm of Dongtai, Dongtai, 224200, China

⁶College of Forestry, Nanjing Forestry University, Nanjing, 210037, China

*Corresponding Authors: Weiwei Lu. Email: wwlu@njfu.edu.cn; Honghua Ruan. Email: hhruan@njfu.edu.cn

Received: 13 November 2019; Accepted: 27 November 2019

Abstract: The priming effect (PE) induced by biochar provides a basis for evaluating its carbon (C) sequestration potential in soils. A 60 days' laboratory incubation was conducted, which involved the amendment of biochar (1% of soil mass) produced from rice straw at 300°C (B300) and 500°C (B500) to young (Y) and old (O) poplar plantation soils, with the aim of studying the responses of biochar-induced PEs to poplar plantation ages. This incubation included six treatments: Y + CK (control), Y + B300, Y + B500, O + CK, O + B300, and O + B500. Carbon dioxide (CO₂) emissions were significantly increased ($p < 0.05$) in the B300 amended soils, while it was decreased in the B500 amended soils compared to the CK. The primed CO₂ emissions were 2.35 times higher in the Y + B300 than the O + B300 treatments, which was measured to be 18.6 and 5.56 mg C·kg⁻¹ with relative PEs of 12.4% and 3.35%, respectively. However, there was little difference between the primed CO₂ emissions in Y + B500 and O + B500 treatments, which were measured to be -24.9 and -29.6 mg·C·kg⁻¹ with relative PEs of -16.6% and -17.8%, respectively. Dissolved organic carbon (DOC) was significantly lower in the young poplar plantation soil than that in the old poplar plantation soil regardless of biochar amendment throughout the incubation, indicating greater C-limit of soil microorganisms in the young poplar plantation soil. Using ¹³C isotope tracing, neither B300 nor B500 decreased native soil-derived DOC, which indicated that the negative B500-induced PEs were not due to a reduction in the availability of native soil-derived C. In conclusion, the response of biochar-induced PEs to poplar plantation age depends on biochar types while soil available C indirectly affects biochar-induced PEs. Further studies should focus on how the interactive effects between soil C availability and microbial community impacts biochar-induced PEs.

Keywords: Biochar; dissolved organic carbon; pyrolysis temperature; poplar plantation age; priming effect

1 Introduction

The soil carbon (C) storage depends on the balance between input and output to the soil. The input of exogenous organic carbon (OC) to soils might change the decomposition of native soil organic carbon (SOC), and thus induce positive or negative priming effects (PEs) [1-4]. The negative PE could mitigate



This work is licensed under a Creative Commons Attribution 4.0 International License, which permits unrestricted use, distribution, and reproduction in any medium, provided the original work is properly cited.

the loss of soil C [5-6], while positive PE could enhance the loss of soil C [7]. Therefore, PE is an important ecological process affecting soil C sequestration.

Biochars are generated through pyrolysis and primarily comprised of recalcitrant compounds [8]. It has been demonstrated that biochar amendment is a potentially effective measure for mitigating carbon dioxide (CO₂) emissions, while improving soil properties [9-12]. Recently, the PEs induced by biochars in soils are garnering the attention of researchers [13-19]. Pyrolysis temperature is a critical factor that influences the properties of biochar, and thus impacts biochar-induced PEs. For example, an earlier study by [20] examined the PEs of a variety of biochar-amended soils, and found that the biochars produced at low temperatures (250°C-400°C) induced positive PEs, while those created at high temperatures (525°C-600°C) induced negative PEs. However, inconsistent results have arisen in recent studies [21-23].

The mechanisms involved in biochar-induced PEs were complicated and have not reached consistency. The positive PEs induced by biochars have generally been ascribed to the stimulation of soil microorganisms following biochar amendment [24], which may be induced by co-metabolism or nutrient (e.g., N or P) mining [25-26]. Positive PEs were often observed at the initial stages of incubation following biochar amendment due to the relief of energy or C-limit of soil microorganisms by the readily available C contained in the biochar [14]. As for biochar-induced negative PEs, there are two types. On one hand, the negative PEs induced by biochars are thought to result from a reduction in the availability of native soil-derived C, due to biochar adsorption [27-29], or the formation of stable aggregates for the longer term addition of biochar [30], which are termed as “negative apparent PEs”. It has been suggested that the negative PEs induced by biochar pyrolyzed at higher temperatures were primarily through sorption, as the specific surface area of biochar increased while mineralizable C decreased with temperature [26,31]. On the other hand, negative PEs were suggested to be induced by changes in soil microbial communities [32], or by substrate switching (also referred to as “preferential substrate utilization” [19]) which means the most labile organic fraction of biochar is preferentially utilized by microbes to temporarily replace the use of native SOC and thus the decomposition of native SOC is decreased [14], which are referred to as “negative real PEs”. Therefore, the biochar-induced negative apparent and real PEs resulted from soil physiochemical and microbial processes, respectively. At present, it is still debating whether biochar-induced negative PEs are mediated by soil physiochemical or microbial processes.

Global C storage has been estimated to be 861 Pg C in forests, which comprises the most extensive and persistent terrestrial C sink [33]. The belowground soil C pool accounts for 44% of the global C storage (383 Pg C) of forests and thus is the most important component of forest C pools [33]. Poplar is one of the most afforested tree species due to its rapid growth and robust adaptability. The poplar plantation area has been estimated to be 7.57 million·hm², accounting for 18.9% of the total arbor plantation areas in China. The C sequestration capacity of soils along a chronosequence of poplar plantations in coastal China was examined by [34], who found that 15 yrs is optimal for the sequestration of atmospheric CO₂, with a mean annual increment of C in soils of 0.573 t·ha⁻¹·yr⁻¹. Furthermore, it was demonstrated that soil attributes such as microbial biomass and C availability were altered with the establishment of poplar plantations [34-35], which might affect PEs following biochar amendment [36]. Therefore, the objectives of this study were as follows: (1) to examine the response of biochar-induced PEs to poplar plantation ages; (2) to explore whether biochar-induced negative PEs resulted from a decrease in the availability of native soil-derived C. To accomplish these goals, we conducted a laboratory incubation experiment through the amendment of the ¹³C spiked biochars pyrolyzed at 300°C and 500°C to soils in young and old poplar plantations. Subsequently, the SOC mineralization as well as C availability were monitored for 60 days during the incubation. Soil respired CO₂ and dissolved organic carbon (DOC) were assigned to native SOC and the applied biochars using ¹³C tracing.

2 Materials and Methods

2.1 Site Description

The study area was at the Dongtai Forest Farm (32°52'37" N, 120°49'44" E), Dongtai City, Jiangsu Province, China, which is in a coastal area of the Yellow Sea and located on the alluvial plains in the middle and lower reaches of the Yangtze River. The area is a transition zone from a north subtropical to warm temperate climate, which is influenced by monsoon. The annual mean temperature, rainfall, and relative humidity is 13.7°C, 1051 mm, and 88.3%, respectively, where the frost-free period and average sunlight duration are 220 d·y⁻¹ and 2169.6 h·y⁻¹, respectively.

2.2 Soil Sampling and Biochar Preparation

Surface soil (0 cm-20 cm) samples were collected from two pure poplar plantations located at the Dongtai Forest Farm. These poplar plantations had been established 4 yrs and 23 yrs (referred to as young and old in this paper) prior to the soil sampling in October, 2016. The understory vegetation in these two plantations was primarily composed of *Humulus scandens* and *Pteris biaurita*. The poplar species was *Populus deltoides* CL'35' and 'I-69', while the afforestation densities were 4 m × 6 m and 6 m × 8 m in the young and old poplar plantations, respectively. The soil samples used in this study possessed a silt loam texture according to the USDA textural classification, with a pH of 7.42 and 8.15 and SOC of 1.40% and 1.45% in the young and old poplar plantation soils, respectively (Tab. 1).

Table 1: Properties of soils in young and old poplar plantations located in a coastal area of Eastern China (means ± standard errors, n = 3)

Poplar plantation	pH	SOC (%)	DOC	C _{mic}	TN (%)	NH ₄ ⁺ -N (mg·kg ⁻¹)	NO ₃ ⁻ -N (mg·kg ⁻¹)	SOC:SON	SOC-δ ¹³ C (‰)	DOC-δ ¹³ C (‰)	Clay (%)	Silt (%)	Sand (%)
Young	(7.42 ± 0.31) a	(1.40 ± 0.08) a	(395 ± 85) b	(493 ± 20) b	(0.13 ± 0.02) a	(3.92 ± 0.36) a	(7.85 ± 0.77) a	(11.6 ± 1.11) a	(-25.1 ± 0.13) b	(-24.4 ± 0.51) a	(11.3 ± 0.29) a	(71.0 ± 0.58) a	(17.7 ± 0.64) a
Old	(8.15 ± 0.02) a	(1.45 ± 0.01) a	(686 ± 12) a	(1023 ± 61) a	(0.10 ± 0.01) a	(2.82 ± 0.45) a	(6.55 ± 0.26) a	(15.0 ± 1.72) a	(-23.6 ± 0.11) a	(-25.3 ± 0.33) a	(11.5 ± 0.58) a	(70.8 ± 0.69) a	(17.7 ± 0.69) a

SOC, soil organic carbon; DOC, dissolved organic carbon; C_{mic}, microbial biomass carbon; TN, total nitrogen; NH₄⁺, ammonium; NO₃⁻, nitrate; SON, soil organic nitrogen. Particle dimensions of clay, silt and sand were < 2 μm, 2-50 μm and 50-2000 μm, respectively.

Values with the same letter were not significantly different, while the values with different letters were significantly different at *p* = 0.05.

The biochar used for this study was prepared using ¹³C labelled rice straw. To obtain the labelled plant material, a pot experiment was conducted at the Xiashu Forest Farm (32°7'19" N, 119°13'53" E), Jurong City, Jiangsu Province, China from June to September 2016 and the labelling method proceeded according to [37]. Following harvest, rice straw was chopped into 3 cm-5 cm pieces, oven-dried, and transferred into a special reactor (China patent No. ZL200920232191.9) for slow-pyrolysis. The reactor was heated by a step-wise procedure, where the temperature was initially set at 200°C, and then incrementally elevated to 250°C, 300°C, 350°C, 400°C, 450°C, and 500°C. The pyrolysis process was terminated when there was no visible smoke emanating from the vent, where the entire process for the final temperatures of 300°C and 500°C continued for about 3.5 and 9.5 h, respectively. Compared with biochar pyrolyzed at 500°C (B500), the biochar pyrolyzed at 300°C (B300) had a lower pH and contained more labile C, which was measured as DOC, O/N-alkyl C and carbonyl C (Tab. 2).

Table 2: Properties of biochars pyrolyzed at 300°C (B300) and 500°C (B500) using rice straw as the raw material (means ± standard errors, n = 3)

Biochar	pH	TC (%)	IC (%)	TN (%)	NH ₄ ⁺ -N (mg·kg ⁻¹)	NO ₃ ⁻ -N (mg·kg ⁻¹)	OC:ON	DOC (mg·kg ⁻¹)	OC-δ ¹³ C (‰)	Ash content (%)	Volatile component (%)	SOC functional groups (%)			
												Alkyl C	O/N-alkyl C	Aryl C	Carbonyl C
B300	(8.23 ± 0.02) b	(57.1 ± 1.67) a	(0.68 ± 0.02) b	(3.98 ± 0.48) a	(27.7 ± 3.50) a	(65.8 ± 6.02) a	(15.2 ± 1.61) a	(5336 ± 109) a	(254 ± 18.7) a	(15.8 ± 0.21) b	(78.9 ± 1.23) a	(25.6 ± 1.50) a	(6.93 ± 0.45) a	(59.4 ± 3.12) b	(8.11 ± 0.64) a
B500	(9.86 ± 0.01) a	(62.7 ± 3.27) a	(1.18 ± 0.06) a	(3.19 ± 0.04) a	(28.8 ± 4.04) a	(11.7 ± 1.33) b	(19.7 ± 1.94) a	(2100 ± 182) b	(284 ± 18.1) a	(22.8 ± 0.41) a	(61.1 ± 7.39) a	(4.15 ± 0.20) b	(2.58 ± 0.19) b	(89.5 ± 1.44) a	(3.74 ± 0.34) b

TC, total carbon; IC, inorganic carbon; TN, total nitrogen; $\text{NH}_4^+\text{-N}$, ammonium nitrogen; $\text{NO}_3^-\text{-N}$, nitrate nitrogen; OC, organic carbon; ON, organic nitrogen; DOC, dissolved organic carbon.

The spectroscopic range of nuclear magnetic resonance for alkyl C, O/N-alkyl C, aryl-C, and carbonyl C was 50 ppm -0 ppm, 95 ppm -50 ppm, 165 ppm -95 ppm and 220 ppm -165 ppm, respectively.

Values with the same letter were not significantly different, while the values with different letters were significantly different at $p = 0.05$.

2.3 Characterization of Soil and Biochar

The soil texture was determined using a laser particle size analyzer (Beckman Coulter, LS, USA) at the Institute of Soil Science, Chinese Academy of Sciences (CAS). Moist soil was dried at 105°C to determine soil moisture content. The pH of the soil was determined with a glass electrode using a soil-to-water ratio of 1:5. Soil microbial biomass was analyzed by chloroform fumigation method. The total C (TC) and total N (TN) contents were determined via an elemental analyzer (PE 2400 II, PekinElmer, USA). The soil inorganic carbon (IC) was measured by the titration method. Soil ammonium nitrogen ($\text{NH}_4^+\text{-N}$) and nitrate nitrogen ($\text{NO}_3^-\text{-N}$) was analyzed by indophenol blue colorimetry and ultraviolet spectrophotometry, respectively. The SOC and SON was calculated as the difference between the TC and IC, and between the TN and IN ($\text{NH}_4^+\text{-N} + \text{NO}_3^-\text{-N}$), respectively.

To analyze the soil DOC, the soil samples were extracted by hot deionized water, filtrated through 0.45 μm filters, and then examined using a TOC analyzer (TOC-L CPH/CPN, Shimadzu, Japan). The DOC extract was initially dried in a freeze drier (FreeZone 2.5 L, Labconco, USA) before the DOC- $\delta^{13}\text{C}$ was determined. To determine the SOC- $\delta^{13}\text{C}$ values, a soil subsample was subjected to acid rinsing to remove the IC according to the method by [38]. The $\delta^{13}\text{C}$ values of both the SOC and DOC were quantified using an isotope ratio mass spectrometer interfaced with an element analyzer (Flash EA δV , Thermo Fisher Scientific, USA) at the Advanced Analysis and Testing Center, Nanjing Forestry University (AATC-NFU).

The pH of the biochar was determined using a glass electrode with a solid-to-water ratio of 1:15 to accommodate the low density of the biochar [24]. The TC, TN, DOC and $\delta^{13}\text{C}$ of the OC and DOC of the biochar were determined using the same methods as for the soil samples. The biochar was combusted at 760°C for 6 h to determine the ash content [39]. The volatile component was determined by combusting the biochar at 950°C for 6 min, and was calculated as the mass difference prior to and following combustion [40]. The quantitative direct-polarization magic angle-spinning (DPMAS) ^{13}C nuclear magnetic resonance (NMR) spectral pattern of the biochar was obtained using a Bruker AV III 400 MHz spectrometer at Nanjing University. Further details regarding this analysis can be found in [41]. The functional groups of the biochar OC were divided into alkyl, O/N-alkyl, aryl and carbonyl C according to [42].

2.4 Incubation Experiment

The incubation included the following six treatments: (1) young poplar plantation soil without biochar amendment (Y + CK), (2) young poplar plantation soil amended with B300 (Y + B300), (3) young poplar plantation soil amended with B500 (Y + B500), (4) old poplar plantation soil without biochar amendment (O + CK), (5) old poplar plantation soil amended with B300 (O + B300), (6) old poplar plantation soil amended with B500 (O + B500). The soil samples and the biochar were crushed and passed through 2 mm and 0.25 mm sieves, respectively. A series of 500 mL flasks containing 100 g of soil sample (on an oven-dried basis) were prepared. The biochar was added to designated flasks at the application rate of 1% of soil mass, which was equivalent to a field application rate of 26 $\text{t}\cdot\text{ha}^{-1}$ (20 cm soil depth, bulk density of 1.30 $\text{g}\cdot\text{cm}^{-3}$), and mixed thoroughly with the soil. The soil moisture was adjusted to 60% water-filled pore space (WFPS) through the addition of deionized water. All of the flasks were covered by aluminum foil with needle-punctured holes to maintain aerobic conditions and then incubated at 25°C in the dark. To maintain a constant soil water content, deionized water was added with a mini-pipette every other day to bring to the original weight during incubation.

Each treatment was repeated in triplicate to quantify the efflux and $\delta^{13}\text{C}$ value of the CO_2 emitted from the soil samples on days 0 (specifically, 1 h after biochar amendment), 1, 3, 7, 14, 30, 45, and 60 during incubation. For gas sampling, each flask was sealed using an airtight stopper. Immediately and after 12 h of enclosure, 25 mL of headspace gas in the flask was sampled using an airtight syringe. To maintain the balance of gas pressure in the flask, an additional 25 mL of high purity nitrogen gas (N_2 , 99.999%) was injected into the flask immediately following gas sampling. The CO_2 concentration was measured using a gas chromatograph equipped with a flame ionization detector (FID) operated at 60°C (Agilent 7890B, Santa Clara, CA, USA). The gas standards of CO_2 were supplied by the National Research Center for Certified Reference Materials, Beijing, China. The $\delta^{13}\text{C}$ values of the emitted CO_2 were measured using an isotope ratio mass spectrometer (Flash δV , Thermo Fisher Scientific, USA) at AATC-NFU. Triplicates in each treatment were destructively sampled on days 0, 1, 7, 30, and 60 to measure the $\delta^{13}\text{C}$ and content of the DOC in soils following the procedures described in Section 2.3.

2.5 Calculations

The CO_2 efflux derived from decomposition of native SOC was calculated using a linear mixing model [43]:

$$f_b = (\delta - \delta_s) / (\delta_b - \delta_s) \quad (1)$$

where δ_s (‰) is the $\delta^{13}\text{C}$ of native SOC, δ_b (‰) is the $\delta^{13}\text{C}$ of OC in biochar, and δ (‰) is the $\delta^{13}\text{C}$ of CO_2 emitted from the biochar-amended soils, which is calculated based on a mass balance equation [44]:

$$\delta = (\delta_2 \times C_2 - \delta_1 \times C_1) / (C_2 - C_1) \quad (2)$$

where C_1 and C_2 is the concentration of CO_2 ($\mu\text{L L}^{-1}$), while δ_1 and δ_2 is the $\delta^{13}\text{C}$ of CO_2 (‰) in gases sampled at zero time and 12 h following flask enclosure, respectively.

Biochar-primed CO_2 emission and the relative PE were calculated according to the method of [45]. The quantity of native soil-derived DOC in biochar-amended soils was calculated using the same method as that of native soil-derived CO_2 efflux.

2.6 Statistical Analysis

All data were reported on an oven-dried soil basis. Repeated measures of ANOVA were employed to examine the differences of total and primed CO_2 effluxes between incubation times. One-way ANOVA was used to examine the differences of total CO_2 efflux, total and native soil-derived DOC between treatments. Least significant difference (LSD) was used for post hoc multiple comparisons if the difference was significant. The independent samples t test was used to examine the differences in magnitudes of the PEs, between the two biochar or soil types, where the significance was set at the $p < 0.05$ level. Distribution normality and variance homogeneity were examined prior to ANOVA. Pearson correlation analysis was carried out to examine the relationship between total or biochar-primed CO_2 efflux and total DOC content. All tests were performed with SPSS 16.0 for Windows (SPSS Inc., Chicago, IL, USA).

3 Results

3.1 Total CO_2 Efflux and Emission

The total CO_2 efflux decreased gradually from the onset of incubation until day 30, which was followed by a slight increase from day 30 to 60 in both the young and old poplar plantation soils (Fig. 1). Compared to CK, the B300 amendment generally significantly increased the total CO_2 efflux in both the young and old poplar plantation soils during incubation (Fig. 1). The B500 amendment had little influence on the total CO_2 efflux in both young and old poplar plantation soils except that it resulted in a decreased effect at the end of incubation in the old poplar plantation soil (Fig. 1). Compared to CK, the B300 was significantly increased, however, the B500 decreased the total CO_2 emission in both the young

and old poplar plantation soils during 60 days of incubation, and there was no difference between young and old poplar plantation soils within the same biochar treatment (Tab. 3).

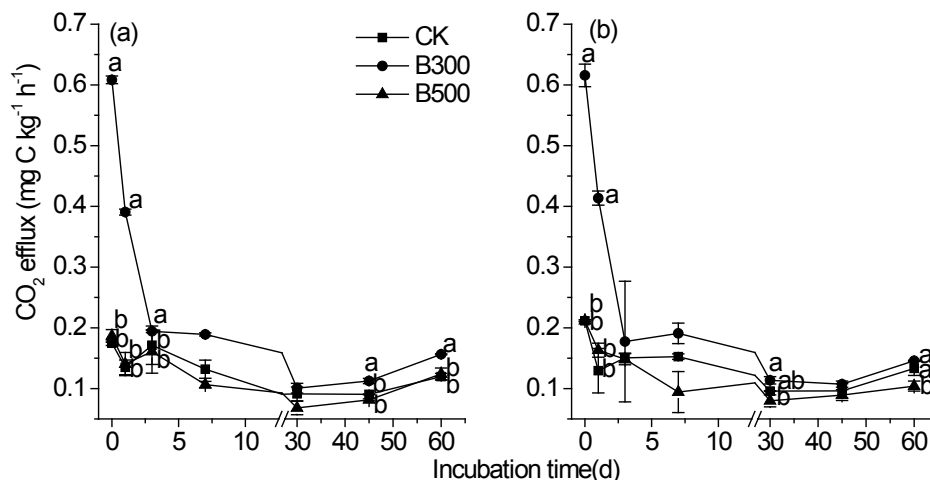


Figure 1: Temporal variations in carbon dioxide (CO₂) efflux from young (a) and old (b) poplar plantation soils amended without (CK) and with biochars pyrolyzed at 300°C (B300) and 500°C (B500) during 60 days of incubation. Different lowercase letters denote significant differences between treatments at the same incubation time at $p < 0.05$. Vertical bars denote the standard error of the mean ($n = 3$)

3.2 Primed SOC Decomposition

Based on the two-component linear mixing model, the total CO₂ efflux was attributed to the CO₂ from the native-soil and that derived from the amended biochar. The B300-primed CO₂ efflux exhibited similar dynamics, while that of B500-primed showed nearly the opposite dynamics of the “W” and “M” shape in the young and old poplar plantation soils, respectively (Fig. 2). The primed CO₂ efflux peaked on day 1 (0.19 and 0.10 mg·C·kg⁻¹·h⁻¹), then decreased sharply to negative values on day 3 (-0.10 and -0.08 mg·C·kg⁻¹·h⁻¹), which was followed by low values ranging from 0 to 0.034 and 0.012 mg·C·kg⁻¹·h⁻¹ from day 7 until the end of incubation in the Y + B300 and O + B300 treatments, respectively (Fig. 2). The primed CO₂ efflux attained the minimum (-0.070 mg·C·kg⁻¹·h⁻¹) and maximum (-0.009 mg·C·kg⁻¹·h⁻¹) on day 3 in the Y + B500 and O + B500 treatments, respectively (Fig. 2). Overall, the B300 amendment induced positive PEs, however, the B500 amendment resulted in negative PEs in both the young and old poplar plantation soils (Tab. 3). The primed cumulative CO₂ emissions from the Y + B300 treatment were 2.35 times higher than that from the O + B300 treatment (18.6 vs. 5.56 mg·C·kg⁻¹), while the difference between the Y + B500 and O + B500 treatments (-24.9 vs. -29.6 mg·C·kg⁻¹) was small (Tab. 3). This corresponded to relative PEs of 12.4% and 3.35% in the Y + B300 and O + B300 treatments, and -16.6% and -17.8% in the Y + B500 and O + B500 treatments, respectively (Tab. 3). Generally, the primed CO₂ emissions accounted for less than 1% of the initial SOC during the 60 days of incubation (Tab. 3).

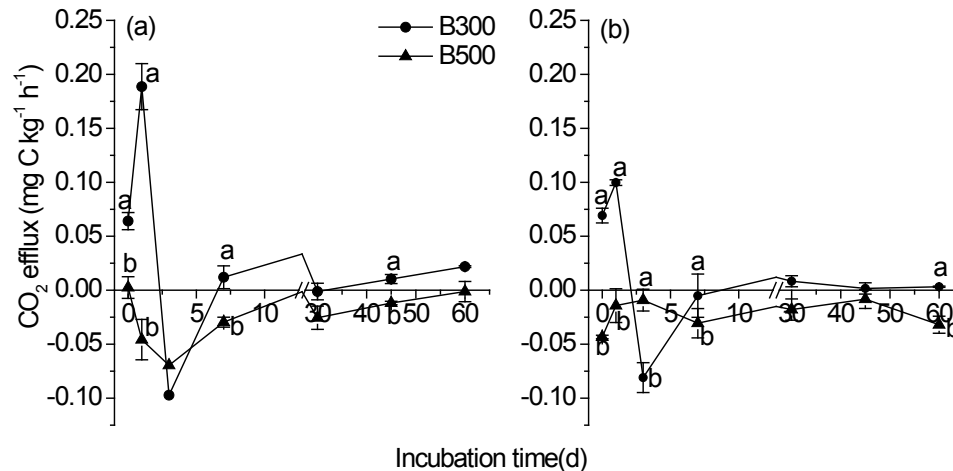


Figure 2: Temporal variations in carbon dioxide (CO_2) efflux primed by biochars pyrolyzed at 300°C (B300) and 500°C (B500) in young (a) and old (b) poplar plantation soils during 60 days of incubation. Different lowercase letters denote significant differences between treatments at the same incubation time at $p < 0.05$. Vertical bars denote the standard error of the mean ($n = 3$)

3.3 DOC Content

Table 3: Carbon dioxide (CO_2) emission and magnitude of priming effect on soil organic carbon (SOC) decomposition induced by biochars pyrolyzed at 300°C (B300) and 500°C (B500) in young (Y) and old (O) poplar plantation soils during 60 days of incubation (means \pm standard errors, $n = 3$)

Treatment	CO_2 emission ($\text{mg}\cdot\text{C}\cdot\text{kg}^{-1}$)				Primed CO_2 emission relative to (%)		
	Total	Native soil-derived	Biochar-derived	Primed by biochar	CO_2 emission in CK	Initial SOC	Initial C_{mic}
Y+CK	(150 \pm 9.98) b A	(150 \pm 9.98) a A	-	-	-	-	-
Y+B300	(210 \pm 4.23) a A	(168 \pm 4.02) a A	(41.9 \pm 0.54) a A	(18.6 \pm 4.02) a A	(12.4 \pm 2.68) a A	(0.13 \pm 0.03) a A	(3.77 \pm 0.82) a A
Y+B500	(136 \pm 5.61) b A	(125 \pm 3.33) b B	(10.6 \pm 2.58) b A	(-24.9 \pm 3.33) b A	(-16.6 \pm 2.22) b A	(-0.18 \pm 0.02) b A	(-5.04 \pm 0.67) b B
O+CK	(166 \pm 8.88) b A	(166 \pm 8.88) a A	-	-	-	-	-
O+B300	(211 \pm 4.96) a A	(172 \pm 1.29) a A	(39.7 \pm 3.81) a A	(5.56 \pm 1.29) a B	(3.35 \pm 0.78) a B	(0.04 \pm 0.01) a B	(0.54 \pm 0.13) a B
O+B500	(142 \pm 1.52) c A	(136 \pm 1.49) b A	(5.79 \pm 0.28) b A	(-29.6 \pm 1.49) b A	(-17.8 \pm 0.90) b A	(-0.20 \pm 0.01) b A	(-2.89 \pm 0.15) b A

C_{mic} , soil microbial biomass carbon; CK, control without biochar amendment.

Within one soil type, the values followed by different lowercase letters were significantly different between biochar types at $p < 0.05$; within one biochar type, the values followed by different uppercase letters were significantly different between soil types at $p < 0.05$.

The DOC content fluctuated in the young poplar plantation soil while it gradually decreased in the old poplar plantation soil during incubation (Figs. 3(a) and 3(b)). The biochar amendment did not show significant influence on the DOC content throughout the incubation in either the young or old poplar plantation soils (Figs. 3(a) and 3(b)). The DOC content of the young poplar plantation soil was significantly lower than that of the old poplar plantation soil (Figs. 3(a) and 3(b); Tab. 4). The correlation between total DOC content and CO_2 efflux (total or biochar-primed) was not significant except that in O + CK treatment (with total CO_2 efflux, $r = 0.977^{**}$, $p < 0.01$, $n = 5$). The portion of native soil-derived DOC was $> 90\%$ in biochar-amended young and old poplar plantation soils throughout the incubation, which indicated that most of the DOC in the soil-biochar mixtures was derived from native soil and thus biochar had a relatively small contribution. The two biochars had no influence on the native soil-derived

DOC throughout the incubation in either soils (Figs. 3(c) and 3(d); Tab. 4), except that B500 significantly decreased it on day 0 compared to CK in the young poplar plantation soil (Figs. 3(c) and 3(d)).

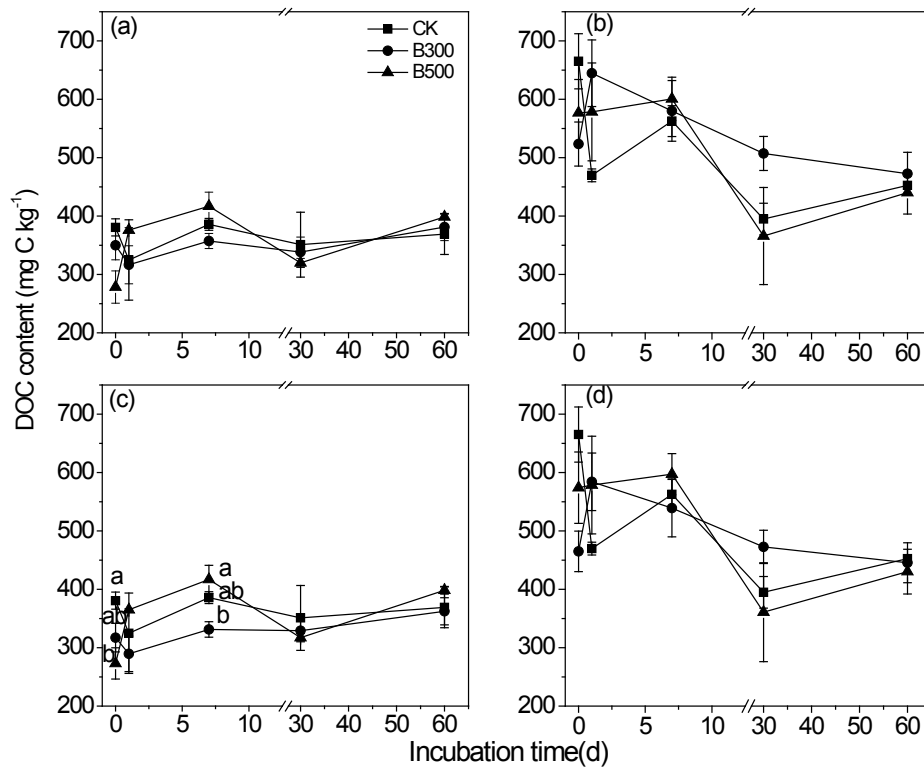


Figure 3: Temporal variations in total dissolved organic carbon (DOC) (a, b) and native soil-derived DOC (c, d) in young (a, c) and old (b, d) poplar plantation soils amended without (CK) and with biochars pyrolyzed at 300°C (B300) and 500°C (B500) during 60 days of incubation. Different lowercase letters denote significant differences between treatments at the same incubation time at $p < 0.05$. Vertical bars denote the standard error of the mean ($n = 3$)

Table 4: Average content of dissolved organic carbon (DOC) and that derived from native soil in young (Y) and old (O) poplar plantation soils amended without (CK) and with biochars pyrolyzed at 300°C (B300) and 500°C (B500) during 60 days of incubation (means \pm standard errors, $n = 3$)

Treatment	Total DOC ($\text{mg} \cdot \text{C} \cdot \text{kg}^{-1}$)	Native soil-derived DOC ($\text{mg} \cdot \text{C} \cdot \text{kg}^{-1}$)
Y + CK	366 ± 17.0 a B	366 ± 17.0 a B
Y + B300	349 ± 4.39 a B	325 ± 5.61 a B
Y + B500	353 ± 3.65 a B	349 ± 3.15 a B
O + CK	513 ± 17.0 a A	513 ± 17.0 a A
O + B300	546 ± 16.0 a A	501 ± 12.5 a A
O + B500	497 ± 38.5 a A	492 ± 38.4 a A

Within one soil type, the values followed by different lowercase letters were significantly different between treatments at $p < 0.05$; within one biochar type, the values followed by different uppercase letters were significantly different between soil types at $p < 0.05$.

4 Discussion

4.1 Magnitudes and Directions of PEs Induced by Biochars Pyrolyzed at 300°C and 500°C

The biochar produced at 300°C generally induced positive PE, while that produced at 500°C induced negative PE in both young and old poplar plantation soils in this study (Fig. 2, Tab. 3), which was consistent with [20]. In contrast, the negative PE induced by biochar produced at lower temperatures (200°C-300°C) [21-22], and positive PE induced by biochar produced at higher temperatures (500°C-600°C) were also reported in recent studies [21,23]. In earlier studies, the magnitudes of biochar-induced PEs were not often quantified [28,30,46]. However, more data on the magnitude of PEs are available (Tab. 5). It was not surprising to find that the magnitudes of PEs had a rather wide range between different studies, as soil and biochar attributes were crucial factors in the control of biochar-induced PEs [15]. The primed native SOC decomposition ranged from -29.6 to 18.6 mg·kg⁻¹, with the relative PEs ranging from -17.8% to 12.4% during the 60 days' incubation period (Tab. 3). Overall, the magnitudes of the biochar-induced PEs in this study were within previously reported ranges.

It is worth noting that the primed CO₂ efflux dropped to negative values on day 3, which was followed by negligible PEs in both Y + B300 and O + B300 treatments (Fig. 2). Previous studies demonstrated that the direction of the PEs might change over the course of the incubation period [15,49-50]. Several studies observed that initial positive biochar-induced PEs diminished over time [20,51]. In particular, a number of studies found that the positive PE was followed by a negative PE in biochar-amended soils [22,52]. It was suggested that several mechanisms involved in PEs might exist simultaneously, with one mechanism being dominant [36]. Furthermore, a succession of mechanisms involved in PEs can occur during incubation [53-54]. Consequently, the negative PEs that appeared on day 3 under the B300-amended soils were most likely due to the shift of dominant mechanisms.

Table 5: Directions and magnitudes of biochar-induced priming effect (PE) in reported studies with different soil and biochar types and incubation durations

Soil type	Biochar type	Incubation time (d)	Primed CO ₂ emission (mg·C·kg ⁻¹ soil)	Relative PE (%)	Primed CO ₂ emission/initial SOC (%)	Method	Reference
Alfisol, Entisol and Mollisol	Grass and wood (250°C, 400°C, 525°C and 650°C)	365	–	-52 – 89	–	No isotope	[20]
Aquic paleudalf (silty loam)	Grass (350°C and 700°C)	87	77.6 – 319	50.9 – 1110	0.8 – 3.3	Isotope	[24]
Silty arable Luvisol	Maize (600°C)	57	–	-24 and -38	–	Isotope	[47]
Silty stagnic Luvisol	Grass (600°C)	37	–	-56	–	Isotope	[32]
Various	Various	365	300	–	–	Meta-analysis	[15]
Various	Crop	–	–	-20.3	–	Meta-analysis	[48]
Sandy loam	Corn straw (500°C)	30	-95.9 – -64.4	-66.9 – -72.0	-1.46 – -0.98	Isotope	[45]
Sandy (Typic Orthods)	Wood (200°C, 300°C, 450°C and 600°C)	About 300 (10 months)	–	-3 – -40	–	Isotope	[22]
Uvisol	Grass, maize straw, sugarcane and peanut shells (300°C, 400°C and 500°C)	80	-135 – 1214	-19.0 – 172	-0.46 – 4.17	Isotope	[21]
Sandy loam	Rice straw (300°C and 500°C)	60	-29.6 – 18.6	-17.8 – 12.4	-0.20 – 0.13	Isotope	This study

CO₂, carbon dioxide; SOC, soil organic carbon.

4.2 Response of B300-Induced Positive PEs to Poplar Plantation Ages

The increased CO₂ emission by B300 amendment in both the young and old poplar plantation soils indicated that soil microbes were activated by B300 (Tab. 3). The positive PEs induced by the B300 were considered to be apparent in this study, which was assumed to be a result of increased maintenance

respiration due to the activation of dormant microorganisms and was supported by the following indicators: (i) The added readily available OC contained in biochar was lower than the initial soil microbial biomass carbon (C_{mic} , 10.8% and 5.22% of C_{mic} in the young and old poplar plantation soils, respectively), which was an insufficient quantity to induce a real PE [36,55]; (ii) The quantity of primed C was lower than that of soil C_{mic} (Tab. 3) [56]. The less available C in young poplar plantation soil (Tab. 1), which primarily resulted from less C input from vegetation, such as litter and root [57], was concurrent with the higher B300-primed extra native soil-derived CO_2 emission when compared with the old poplar plantation soil (Tab. 3). Therefore, the soil microorganisms in the studied soils were most probably C or energy-limited, and the stronger C-limit or greater activation of soil microbes by B300 was speculated to be responsible for the stronger positive PEs in the young poplar plantation soil. The limiting effect of available C on SOC decomposition in the subsoil was also reported by [5]. Our interpretation was consistent with [14] who found that soil having less easily mineralizable SOM was more susceptible to SOC decomposition through the addition of biochar. Furthermore, this interpretation was consistent with [29,58], both of which found negative PEs in soils with relatively high mineralizable SOC. Therefore, our results supported the notion that the easily available C contained in biochar pyrolyzed at low temperatures could alleviate, to some extent, the C- or energy-limit of soil resident microorganisms, and supported the hypothesis that the mineralizability of SOC impacts the magnitude and direction of biochar-induced PEs [14].

4.3 Effects of B500 on Native Soil-Derived DOC and Implications for the Mechanisms Involved in B500-Induced Negative PEs

It has been commonly suggested that the negative PEs induced by biochar pyrolyzed at high temperatures resulted from the decrease of native soil-derived C availability [26,29]. However, the data collected in this study did not support this hypothesis. We did not find a significant decrease of native soil-derived DOC in the B500-amended soils compared to the CK using ^{13}C isotope tracing (Figs. 3(c) and 3(d)). This indicated that the decreased availability of native soil-derived C due to adsorption or soil aggregate formation was not responsible for the negative PEs induced by B500. Our finding was consistent with [32], who also found that the negative PEs induced by biochars were primarily due to reduced microbial activity and biomass instead of adsorption of DOC by biochars. However, our results contradicted our previous study in a sandy loam arable soil, where we found that biochar derived from corn stover produced at 500°C significantly decreased native soil-derived DOC [29]. Furthermore, a recent study concluded that the sorptive protection of DOC was responsible for the majority of negative PEs induced by biochars based on adsorption isotherm experiments, as well as the co-location of native SOC on biochar surfaces as shown by nanoSIMs [59]. These inconsistencies might have been due to the differences of soil and biochar properties and their subsequent interactions in the reported studies. In this study, the small proportion of biochar within the soil matrix might have been responsible for the lack of adsorption by B500 [60]. In addition, the relatively higher SOC content (1.40% and 1.45% in the young and old poplar plantation soils respectively) in the studied soils might also contribute, since previous investigations revealed that the adsorption affinity of biochar decreased with higher solute concentrations [60-61]. Therefore, the B500-induced negative PEs were indirectly demonstrated to be due to the change of soil microbial community in this study, which warrants further conformation in the future studies.

5 Conclusions

Rice straw-derived biochar pyrolyzed at 300°C and 500°C induced positive and negative PEs, respectively, in amended poplar plantation soils in a coastal area of Eastern China. Young poplar plantation soil was more vulnerable to native SOC loss due to stronger C-limit of soil microorganisms when amended with biochar pyrolyzed at 300°C. In contrast, the negative PEs induced by biochar pyrolyzed at 500°C were similar in young and old poplar plantation soils. ^{13}C analysis indicated that negative PEs induced by biochar pyrolyzed at 500°C was not due to the decrease of native soil-derived C availability. In conclusion, the response of biochar-induced PEs to poplar plantation ages depends on biochar's pyrolysis temperatures while soil available C indirectly affects biochar-induced PEs.

Acknowledgement: This work was supported by National Priority Research and Development Program of China (2016YFD0600204), National Natural Science Foundation of China (41701264), Natural Science Foundation of Jiangsu Province, China (BK20170931), Natural Science Research Program (16KJB210005), Overseas Training Program and Priority Academic Program Development Funds (PAPD) of Jiangsu Higher Education Institutions. We thank Mr. Sun and Mr. Tu from Xiashu, Jiangsu Province, China for their assistance in rice planting.

Conflicts of Interest: The authors declare that they have no conflicts of interest to report regarding the present study.

References

1. Bingeman, C. W., Varner, J. E., Martin, W. P. (1953). The effect of the addition of organic materials on the decomposition of an organic soil. *Soil Science Society of America Proceedings*, 29, 692-696.
2. Kuzyakov, Y., Friedel, J. K., Stahr, K. (2000). Review of mechanism and quantification of priming effects. *Soil Biology and Biochemistry*, 32, 1485-1498.
3. Ma, Y. P., Zhang, Z. J., Su, T. Q., Busso, C. A., Johnston, E. R. et al. (2018). Experimental evidence of soil bacteria abundance as the primary driver of rhizosphere priming effect. *Phyton-International Journal of Experimental Botany*, 87, 286-291.
4. Ji, Y., Liu, P. F., Conrad, R. (2018). Response of fermenting bacterial and methanogenic archaeal communities in paddy soil to progressing rice straw degradation. *Soil Biology and Biochemistry*, 124, 70-80.
5. Fontaine, S., Barot, S., Barré, P., Bdioui, N., Mary, B. et al. (2007). Stability of organic carbon in deep soil layers controlled by fresh carbon supply. *Nature*, 450, 277-280.
6. Fontaine, S., Henault, C., Aamor, A., Bdioui, N., Bloor, J. M. G. et al. (2011). Fungi mediate long term sequestration of carbon and nitrogen in soil through their priming effect. *Soil Biology and Biochemistry*, 43, 86-96.
7. Paterson, E., Sim, A., Davidson, J., Daniell, T. J. (2016). Arbuscular mycorrhizal hyphae promote priming of native soil organic matter mineralisation. *Plant and Soil*, 408, 243-254.
8. Baldock, J. A., Smernik, R. J. (2002). Chemical composition and bioavailability of thermally, altered *Pinus resinosa* (Red Pine) wood. *Organic Geochemistry*, 33, 1093-1109.
9. Sun, H. J., Lu, H. Y., Feng, Y. F. (2019a). Greenhouse gas emissions vary in response to different biochar amendments: an assessment based on two consecutive rice growth cycles. *Environmental Science and Pollution Research*, 26, 749-758.
10. Sun, H. J., Zhang, H. C., Shi, W. M., Zhou, M. Y., Ma, X. F. (2019b). Effect of biochar on nitrogen use efficiency, grain yield and amino acid content of wheat cultivated on saline soil. *Plant Soil and Environment*, 65, 83-89.
11. Chu, L., Hennayake, H. M. K. D., Sun, H. J. (2019). Biochar effectively reduces ammonia volatilization from nitrogen-applied soils in tea and bamboo plantations. *Phyton-International Journal of Experimental Botany*, 88(3), 261-267.
12. Liu, Q., Liu, B. J., Zhang, Y. H., Hu, T. L., Lin, Z. B. et al. (2019). Biochar application as a tool to decrease soil nitrogen losses (NH₃ volatilization, N₂O emissions, and N leaching) from croplands: options and mitigation strength in a global perspective. *Global Change Biology*, 25, 2077-2093.
13. Whitman, T., Enders, A., Lehmann, J. (2014a). Pyrogenic carbon additions to soil counteract positive priming of soil carbon mineralization by plants. *Soil Biology and Biochemistry*, 73, 33-41.
14. Whitman, T., Zhu, Z., Lehmann, J. (2014b). Carbon mineralizability determines interactive effects on mineralization of pyrogenic organic matter and soil organic carbon. *Environmental Science and Technology*, 48, 13727-13734.
15. Maestrini, B., Nannipieri, P., Abiven, S. (2015). A meta-analysis on pyrogenic organic matter induced priming effect. *Global Change Biology Bioenergy*, 7, 577-590.
16. Sheng, Y. Q., Zhan, Y., Zhu, L. Z. (2016). Reduced carbon sequestration potential of biochar in acidic soil. *Science of Total Environment*, 572, 129-137.

17. Luo, X. X., Wang, L. Y., Liu, G. C., Wang, X., Wang, Z. Y. et al. (2016). Effects of biochar on carbon mineralization of coastal wetland soils in the yellow river delta, China. *Ecological Engineering*, 94, 329-336.
18. Cui, J., Ge, T., Kuzyakov, Y., Nie, M., Fang, C. M. et al. (2017). Interactions between biochar and litter priming: a three-source ^{14}C and $\delta^{13}\text{C}$ partitioning study. *Soil Biology and Biochemistry*, 104, 49-58.
19. Zimmerman, A. R., Ouyang L. (2019). Priming of pyrogenic C (biochar) mineralization by dissolved organic matter and vice versa. *Soil Biology and Biochemistry*, 130, 105-112.
20. Zimmerman, A. R., Gao, B., Ahn, M. Y. (2011). Positive and negative carbon mineralization priming effects among a variety of biochar-amended soils. *Soil Biology and Biochemistry*, 43, 1169-1179.
21. Yu, Z., Chen, L., Pan, S., Li, Y., Kuzyakov, Y. et al. (2018). Feedstock determines biochar-induced soil priming effects by stimulating the activity of specific microorganisms. *European Journal of Soil Science*, 69, 521-534.
22. Gibson, C., Hatton, P. J., Bird, J. A., Nadelhoffer, K., Le Moine, J. et al. (2018). Tree taxa and pyrolysis temperature interact to control pyrogenic organic matter induced native soil organic carbon priming. *Soil Biology and Biochemistry*, 119, 174-183.
23. Purakayastha, T. J., Das, K. C., Gaskin, J., Keith, H., Smith, J. L. et al. (2016). Effect of pyrolysis temperatures on stability and priming effects of C3 and C4 biochars applied to two different soils. *Soil Tillage and Research*, 155, 107-115.
24. Luo, Y., Durenkamp, M., De Nobili, M., Lin, Q., Brookes, P. C. (2011). Short term soil priming effects and the mineralisation of biochar following its incorporation to soils of different pH. *Soil Biology and Biochemistry*, 43, 2304-2314.
25. Ramirez, K. S., Craine, J. M., Fierer, N. (2012). Consistent effects of nitrogen amendments on soil microbial communities across biomes. *Global Change Biology*, 18, 1918-1927.
26. Whitman, T., Singh, B. P., Zimmerman, A. R. (2015). Priming effects in biochar-amended soils: implications of biochar-soil organic matter interactions for carbon storage. In: Lehmann, J., Joseph, S. (Eds.), *Biochar for Environmental Management: Science, Technology and Implementation*, pp. 455-488. Earthscan from Routledge,
27. Kimetu, J. M., Lehmann, J. (2010). Stability and stabilisation of biochar and green manure in soil with different organic carbon contents. *Australian Journal of Soil Research*, 48, 577-585.
28. Cross, A., Sohi, S. P. (2011). The priming potential of biochar products in relation to labile carbon contents and soil organic matter status. *Soil Biology and Biochemistry*, 43, 2127-2134.
29. Lu, W. W., Ding, W. X., Zhang, H. J., Li, Y., Luo, J. F. et al. (2014). Biochar suppressed the decomposition of organic carbon in a cultivated sandy loam soil: A negative priming effect. *Soil Biology and Biochemistry*, 76, 12-21.
30. Liang, B. Q., Lehmann, J., Sohi, S. P., Thies, J. E., O'Neill, B. et al. (2010). Black carbon affects the cycling of non-black carbon in soil. *Organic Geochemistry*, 41, 206-213.
31. Kasozi, G. N., Zimmerman, A. R., Nkedi-Kizza, P., Gao, B. (2010). Catechol and humic acid sorption onto a range of laboratory-produced black carbons (biochars). *Environmental Science and Technology*, 44, 6189-6195.
32. Bamminger, C., Zaiser, N., Zinsser, P., Lamers, M., Kammann, C. et al. (2014a). Effects of biochar, earthworms, and litter addition on soil microbial activity and abundance in a temperate agricultural soil. *Biology and Fertility of Soils*, 50, 1189-1200.
33. Pan, Y. D., Birdsey, R. A., Fang, J. Y., Houghton, R., Kauppi, P. E. et al. (2011). A large and persistent carbon sink in the world's forests. *Science*, 333, 988-993.
34. Wang, G. B., Deng, F. F., Xu, W. H., Chen, H. Y. H., Ruan, H. H. (2016). Poplar plantations in coastal China: towards the identification of the best rotation age for optimal soil carbon sequestration. *Soil Use and Management*, 32, 303-310.
35. Ge, Z. W., Fang, S. Y., Chen, H. Y. H., Zhu, R. W., Peng, S. L. et al. (2018). Soil aggregation and organic carbon dynamics in poplar plantations. *Forests*, 9(508).
36. Blagodatskaya, E., Kuzyakov, Y. (2008). Mechanisms of real and apparent priming effects and their dependence on soil microbial biomass and community structure: critical review. *Biology and Fertility of Soils*, 45, 115-131.
37. Baumann, K., Marschner, P., Kuhn, T. K., Smernik, R. J., Baldock, J. A. (2011). Microbial community structure and residue chemistry during decomposition of shoots and roots of young and mature wheat (*Triticum aestivum* L.) in sand. *European Journal of Soil Science*, 62, 666-675.

38. Midwood, A. J., Boutton, T. W. (1998). Soil carbonate decomposition by acid has little effect on $\delta^{13}\text{C}$ or of organic matter. *Soil Biology and Biochemistry*, 30, 1301-1307.
39. Novak, J. M., Busscher, W. J., Laird, D. L., Ahmedna, M., Watts, D. W. et al. (2009). Impact of biochar amendment on fertility of a southeastern coastal plain soil. *Soil Science*, 174, 105-112.
40. ASTM D1762-84. (2001). Standard test method for chemical analysis of wood charcoal.
41. Lu, W. W., Ding, W. X., Zhang, J. H., Zhang, H. J., Luo, J. F. et al. (2015). Nitrogen amendment stimulated decomposition of maize straw-derived biochar in a sandy loam soil: a short-term study. *PLoS One*, 10, e0133131.
42. Solum, M. S., Pugmire, R. J., Grant, D. M. (1989). ^{13}C solid-state NMR of Argonne premium coals. *Energy and Fuels*, 3, 187-193.
43. Amelung, W., Brodowski, S., Sandhage-Hofmann, A., Bol, R. (2008). Combining biomarker with stable isotope analyses for assessing the transformation and turnover of soil organic matter. In: Donald, L.S. (Ed.), *Advances in agronomy*, pp. 155-250. Burlington, Academic Press,
44. Balesdent, J., Mariotti, A. (1996). Measurement of soil organic matter turnover using ^{13}C natural abundance, in: Boutton, T. W., Yamasaki, S. (Eds.), *Mass Spectrometry of Soils*. New York, Marcel Dekker, 83-111.
45. Lu, W. W., Zhang, H. L. (2015). Response of biochar induced carbon mineralization priming effects to additional nitrogen in a sandy loam soil. *Applied Soil Ecology*, 96, 165-171.
46. Kuzyakov, Y., Subbotina, I., Chen, H. Q., Bogomolova, I., Xu, X. L. (2009). Black carbon decomposition and incorporation into soil microbial biomass estimated by ^{14}C labeling. *Soil Biology and Biochemistry*, 41, 210-219.
47. Bamminger, C., Marschner, B., Jüschke, E. (2014b). An incubation study on the stability and biological effects of pyrogenic and hydrothermal biochar in two soils. *European Journal of Soil Science*, 65, 72-82.
48. Wang, J. Y., Xiong, Z. Q., Kuzyakov, Y. (2015). Biochar stability in soil: meta-analysis of decomposition and priming effects. *Global Change Biology Bioenergy*, 8, 512-523.
49. Maestrini, B., Herrmann, A. M., Nannipieri, P., Schmidt, M. W. I., Abiven, S. (2014). Ryegrass-derived pyrogenic organic matter changes organic carbon and nitrogen mineralization in a temperate forest soil. *Soil Biology and Biochemistry*, 69, 291-301.
50. Weng, Z. H., Van Zwieten, L., Singh, B. P., Kimber, S., Morris, S. et al. (2015). Plant-biochar interactions drive the negative priming of soil organic carbon in an annual ryegrass field system. *Soil Biology and Biochemistry*, 90, 111-121.
51. Singh, B. P., Cowie, A. L. (2014). Long-term influence of biochar on native organic carbon mineralisation in a low-carbon clayey soil. *Scientific Reports*, 4, 3687.
52. Ye, R., Doane, T. A., Morris, J., Horwath, W. R. (2015). The effect of rice straw on the priming of soil organic matter and methane production in peat soils. *Soil Biology and Biochemistry*, 81, 98-107.
53. Fontaine, S., Mariotti, A., Abbadie, L. (2003). The priming effect of organic matter: a question of microbial competition? *Soil Biology and Biochemistry*, 35, 837-843.
54. Kuzyakov, Y., Bol, R. (2006). Sources and mechanisms of priming effect induced in two grassland soils amended with slurry and sugar. *Soil Biology and Biochemistry*, 38, 747-758.
55. Blagodatskaya, E., Yuyukina, T., Blagodatsky, S., Kuzyakov, Y. (2011). Three-source-partitioning of microbial biomass and of CO_2 efflux from soil to evaluate mechanisms of priming effects. *Soil Biology and Biochemistry*, 43, 778-786.
56. Kuzyakov, Y. (2010). Priming effects: interactions between living and dead organic matter. *Soil Biology and Biochemistry*, 42, 1363-1371.
57. Zhang, Y. L., Chen, L. J., Chen, X. H., Tan, M. L., Duan, Z. H. et al. (2015). Response of soil enzyme activity to long-term restoration of desertified land. *Catena*, 133, 64-70.
58. Keith, A., Singh, B., Singh, B. P. (2011). Interactive priming of biochar and labile organic matter mineralization in a smectite-rich soil. *Environmental Science and Technology*, 45, 9611-9618.
59. DeCiucies, S., Whitman, T., Woolf, D., Enders, A., Lehmann, J. (2018). Priming mechanisms with additions of pyrogenic organic matter to soil. *Geochimica et Cosmochimica Acta*, 238, 329-342.
60. Dempster, D. N., Gleeson, D. B., Solaiman, Z. M., Jones, D. L., Murphy, D. V. (2012). Decreased soil microbial biomass and nitrogen mineralisation with eucalyptus biochar addition to a coarse textured soil. *Plant*

and Soil, 354, 311-324.

61. Cornelissen, G., Gustafsson, Ö. (2004). Sorption of phenanthrene to environmental black carbon in sediment with and without organic matter and native sorbates. *Environmental Science and Technology*, 38, 148-155.